SCIENCE CHINA
Technological Sciences

• Article •

July 2016 Vol.59 No.7: 1130–1136
doi: 10.1007/s11431-016-6029-y

An analysis of the correlation between the fluxes of high-energy electrons and low-middle-energy electrons in the magnetosphere

LI ChenFang[1], ZOU Hong[1*], ZONG QiuGang[1], JIA XiangHong[2], CHEN HongFei[1], SHI WeiHong[1] & YU XiangQian[1]

[1] *Institute of Space Physics and Applied Technology, School of Earth and Space Science, Peking University, Beijing 100871, China;*
[2] *State Key Laboratory of Space Medicine Fundamentals and Application, Chinese Astronaut Research and Training Center, Beijing 100093, China*

Received September 23, 2015; accepted January 15, 2016; published online March 11, 2016

The variation of the flux of energetic electrons in the magnetosphere has been proven to be strongly related to the solar wind speed. Observations of GEO orbit show that the flux of low-energy electrons is not only modulated by the solar wind speed, but, if a time delay is added, is also positively correlated to the flux of high-energy electrons. This feature provides a possible method to forecast the flux of high-energy electrons in GEO orbit. In this study, the correlations of the fluxes between the high-energy electrons and low-middle-energy electrons obtained at different L values and in different orbits are investigated to develop the application of this feature. Based on the analysis of long–term data observed by NOAA POES and GOES, the correlations between the fluxes of high-energy electrons and low–middle–energy electrons are good enough at different L values and in different orbits in quiet time, but this correlation is strongly affected by CME–driven geomagnetic storms.

magnetosphere, high-energy electrons, low-middle energy electrons, forecast model

Citation: Li C F, Zou H, Zong Q G, et al. An analysis of the correlation between the fluxes of high-energy electrons and low-middle-energy electrons in the magnetosphere. Sci China Tech Sci, 2016, 59: 1130–1136, doi: 10.1007/s11431-016-6029-y

1 Introduction

The variation of the flux of high-energy electrons in the magnetosphere is both significant and influenced by various factors. Because high-energy electrons, as an important part of the space environment, strongly threaten the safety of spacecraft near-Earth, acceleration mechanism of the high-energy electrons in the magnetosphere has become a hot topic in space physical research. Several theories have been proposed to interpret some of the observations. For example, it is widely accepted that VLF (very low frequency) wave-particle interaction is an acceleration mechanism, based on the fact that the frequency range of VLF waves covers the cyclotron frequencies of electrons in the magnetosphere: therefore, cyclotron resonance easily occurs [1]. Another example is the theory of ULF (ultra low frequency) wave-particle interaction, which has been proposed for some observations that cannot be explained well by VLF wave-particle interaction due to its low acceleration efficiency [2,3]. Many other wave–particle interactions have been investigated in theoretical study and data analysis [4–6]. Due to the limitation of the existing observation methods and the complexity of this research, the current understanding of the mechanisms of magnetospheric electron acceleration cannot form the basis for a pure theoretical model for high-energy electron forecasting. Nonetheless, the need for such a model in human space activities is urgent. Some models based on both statistical data and physical mechanisms have been

*Corresponding author (email: hongzou@pku.edu.cn)

proposed: using the electron radial diffusion function, an electron flux model was built that gives good results for the simulation of high-energy electrons flux during quiet time [7]; a prediction generated by a model that combines solar wind and electron flux shows a linear correlation coefficient with the observation up to 0.9 [8–10]; a short-term forecast was produced by a model based on the relationship between geomagnetic activity and electron flux [11]; an empirical equations derived from long-term observation of the relation between K_p index and electron flux was used to build a forecast model [12].

The flux of MeV electrons in GEO orbit has been found to be strongly related to the solar wind speed [13]. Using the observations of 50 keV–6 MeV electrons measured by the LANL satellites in GEO orbit, it is further indicated that after adding a time delay, the flux of low-middle-energy electrons would be well correlated to the flux of high-energy electrons, in addition, the time delay, which is affected by solar wind conditions, shows a tendency to increase as the energy gap between low-middle-energy electrons and high-energy electrons increases [14]. That the time delay between the fluxes of hundreds of keV electrons and several MeV electrons could reach the order of days, provides a good foundation for a forecast model. However, as pointed out by Li et al. [14], the correlation between the low-mid- dle-energy and high-energy electrons in GEO orbit could not be applied to other orbits used to prove whether the high-energy electrons are generated by the local acceleration mechanism of the VLF wave-particle interaction, or by the inward diffusion from the outer region of the magnetosphere.

It is interesting to speculate whether the correlation between the low-middle-energy and high-energy electrons could be applied to other orbits. In this study, the flux of >2.0 MeV electrons measured by NOAA-GOES satellites in GEO orbit and the flux of 30–100 keV electrons measured by NOAA-POES satellites in LEO orbit are compared. The correlations between the flux of low-middle-energy and high-energy electrons at the same L values in different orbits and at different L values in different orbits are also investigated. The data used in this study and the method of the data analysis are introduced in Section 2. Sections 3 and 4 contain the results and discussions. The main point of view in this study is summarized in Section 5.

2 Data and data processing

The space environment monitor (SEM-2) onboard the NOAA-POES-15 satellite can measure the electron fluxes in three integrated energy ranges (>30 keV, >100 keV and >300 keV) as well as the proton fluxes in five integrated energy ranges (>30 keV, >80 keV, >240 keV, >800 keV and >2500 keV). The flux of 30–100 keV electrons can be derived from the fluxes of >30 keV and >100 keV electrons. This proton flux data can be used to rule out proton contamination in the electron flux. It is proved that the flux of the 80–240 keV protons which contaminate the three electron channels is generally two magnitudes less than the electron flux, even during solar proton events (SPEs) [15]. Therefore, a convenient method to get rid of the proton contamination from the electron flux is simply removing the data points when the difference between the electron and proton flux is less than one order of magnitude. As satellites in polar orbits, NOAA-POES craft observe the particles at all the L values of the outer radiation belt, not just the L value in GEO orbit. Usually the NOAA-POES satellites sample the particles at a certain L value four times during one orbit, locating in the southern ascending, northern ascending, northern descending and southern descending orbit branches. To minimize variations caused by local time and geomagnetic field differences, all the data points at the same L value obtained in one day are averaged. This means that the time resolution of our data is a day.

The NOAA-GOES satellites can measure the flux of >2.0 MeV electrons in GEO orbit. To decrease the variations due to the local time effect, the daily averaged flux of >2.0 MeV electrons is used in this study, and the L value for the data is considered to be 6.6.

As an indicator of the space environment activity, the Dst index is selected to study the effect of space environment on electron flux. The Dst index is available in the website of World Data Center for Geomagnetism, Kyoto (URL: http://wdc.kugi.kyoto-u.ac.jp/).

The fluxes of the electrons in different energy ranges simultaneously observed by NOAA-POES and NOAA-GOES satellites are available from January 1999 to June 2004. Figure 1 shows the electron fluxes in two different energy ranges measured by POES-15 and GOES-8–GOES-11 during the second half of 1999. The upper panel shows the temporal variation of the daily averaged flux of 30–100 keV electrons observed at L = 6.6 by POES-15. For comparison, the lower panel shows the daily averaged flux of >2 MeV electrons measured by GOES in GEO orbit (L~6.6) in the same time period. The two curves show similar temporal variation. The vertical dashed lines in Figure 1 mark several obvious peaks or valleys. It can be seen that the peaks and valleys in the curve of the 30–100 keV electrons (chosen to represent the low-middle energy electron) appear several days ahead of those in curve of the>2 MeV (chosen to represent the high-energy electrons) .

3 Results

According to the comparison of the electron fluxes obtained at the same L value (Figure 1), the temporal variation of the low-middle-energy electron flux is almost consistent with that of the high-energy electron flux with a time delay at a magnitude of days, including the data gathered in different

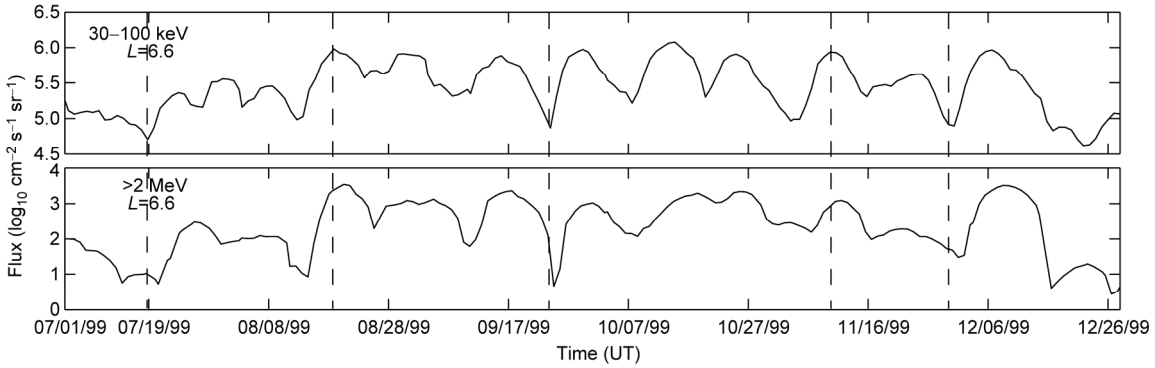

Figure 1 The temporal variations of the fluxes of the low-middle and high-energy electrons observed at *L*~6.6 in the second half of 1999. The upper panel shows the 30–100 keV electrons obtained by POES. The lower panel shows >2 MeV electrons measured by GOES.

locations (low-middle-energy electrons from the polar regions and high-energy electrons from the equatorial region). To confirm the correlation between the low-middle-energy electrons and high-energy electrons, electron observations at several *L* values over different orbits in a long time period should be compared. In this study, a method similar to Li [14] was used to calculate the correlation coefficients that represent the consistency of the two electron observations. First, a time delay was added to the low-middle-energy electron flux and the correlation coefficient with the high-energy electron flux was calculated; next, the time delay was changed and the first step was repeated; last, the maximal correlation coefficient and the corresponding time delay were found.

3.1 Data analysis for the same *L* value in different orbits

The 30–100 keV electrons at *L*=6.6 obtained by POES in polar orbits were compared with the >2.0 MeV electrons measured by GOES in GEO orbit. The data from January 1999 to June 2004 were separately analyzed every 6 months (Table 1).

As shown in Table 1 the correlation coefficients for most of data sets are above 0.6 and some are above 0.8, which means the consistency of the two electron observations is good in most of the time, although the correlation coefficients are smaller than the results derived from the data obtained in the same orbit (above 0.8 [14]). With the data sets in Table 1, the times of the two parameters (time delay and correlation coefficient) were counted and they respectively fall into sets of data bins 0–1, 1–2, 2–3, ···, 9–10 days and 0–0.1, 0.1–0.2, 0.2–0.3,···, 0.9–1.0. Figure 2, which contains the distributions of two parameters, shows that they generally follow the normal distribution. The highest occurrence of the best time delay is in the bin of 2–3 days—slightly longer than the results given by Li et al. [14]. However, in Li's research, the highest and lowest energy ranges of the electron data are 1.1–1.5 MeV and 50–75 keV respectively, in other words, the energy difference in Li's research is smaller than in this study. Therefore, the results shown in Table 1 are reasonable.

Table 1 The correlation results of the electron data at the same *L* value in different orbits

Time range	Time delay (days)	Correlation coefficient
1999.01–1999.06	2.42	0.77
1999.07–1999.12	1.58	0.86
2000.01–2000.06	2.80	0.64
2000.07–2000.12	4.04	0.48
2001.01–2001.06	3.25	0.64
2001.07–2001.12	2.42	0.53
2002.01–2002.06	3.13	0.57
2002.07–2002.12	2.42	0.75
2003.01–2003.06	2.46	0.80
2003.07–2003.12	1.75	0.73
2004.01–2004.06	2.12	0.67

3.2 Data analysis for different *L* values in different orbits

To study the influence of *L* value on the correlation between the low-middle-energy and high-energy electron fluxes, the 30–100 keV electron fluxes observed at *L*=5.0, *L*=3.5 by POES are compared with the flux of >2.0 MeV electrons measured by GOES at *L*=6.6. Table 2 shows the results in the same time periods as shown in Table 1.

According to the results listed in Tables 1 and 2, as *L* value decreases from *L*=6.6, so do the correlation coefficient and the variation range of the best time delay. The variations of the best time delay are smaller for the time periods with large correlation coefficient, such as the data set 2003.01–2003.06. For the time periods with small correlation coefficient, such as the data set 2000.07–2000.12, the correlation coefficient is below 0.3 and the best time delay is even longer than 5 days. This means there is no correlation between the two sets of electron data.

3.3 Data analysis for the long term data sets

For comparison, the correlation coefficients and the best

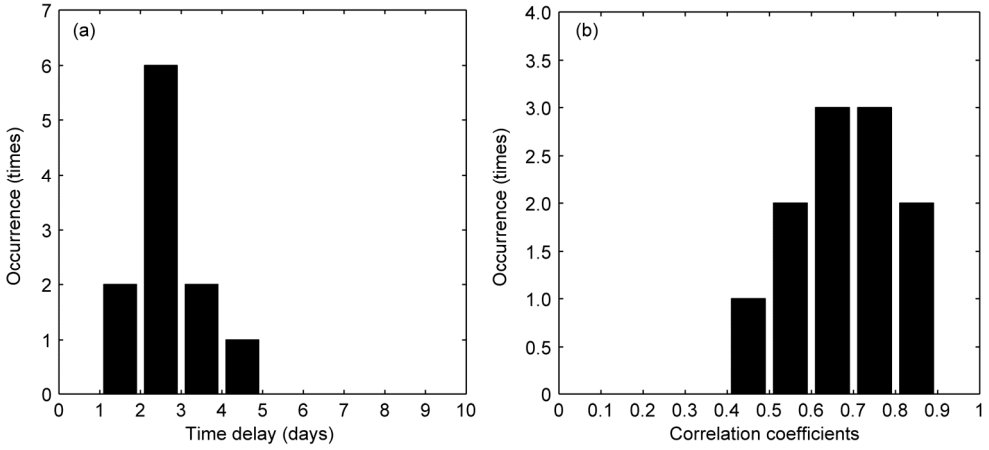

Figure 2 The distributions of the time delays (a) and correlation coefficients (b) for the data sets in Table 1.

Table 2 The correlation results of the electron data at different *L* values in different orbits

Time range	Time delay (days) *L*=5.0	Correlation coefficient *L*=5.0	Time delay (days) *L*=3.5	Correlation coefficient *L*=3.5
1999.01–1999.06	2.88	0.70	1.96	0.64
1999.07–1999.12	1.86	0.82	0.58	0.76
2000.01–2000.06	3.29	0.57	4.63	0.38
2000.07–2000.12	>5	0.29	>5	0.27
2001.01–2001.06	3.17	0.59	2.42	0.57
2001.07–2001.12	4.00	0.35	3.29	0.18
2002.01–2002.06	4.38	0.55	>5	0.54
2002.07–2002.12	3.25	0.71	3.63	0.54
2003.01–2003.06	2.71	0.72	2.38	0.71
2003.07–2003.12	2.50	0.66	2.42	0.45
2004.01–2004.06	2.33	0.63	1.96	0.66

time delays for the long–term data sets were also calculated. Table 3 shows the results for three 36-month data sets (1999–2003). The best time delays for all the data sets are between 2 and 3 days, and the correlation coefficients are all above 0.65. It can be seen that although the correlation coefficients for the long-term data sets are slightly smaller than the best correlation coefficients for the short-term data sets, the best time delays for the long-term data sets are much more stable. This difference could be due to space environment disturbances. For extreme conditions, we analyzed the correlation coefficient and the best time delay for the data set with all available data during 1999.01–2004.06 (66 months). The best time delay is 2.28 days and the correlation coefficient is 0.72.

Table 3 The results of long term date sets

Time range	Time delay (days)	Correlation coefficient
1999.01–2001.12	2.38	0.69
2000.01–2002.12	2.88	0.65
2001.01–2003.12	2.58	0.75

4 Discussion

4.1 The factors that affect the correlation coefficient

As shown in Table 1, the correlation coefficients of some data sets are very low. For example, the correlation coefficient between the high-energy electron flux at *L*=6.6 and the low-middle-energy electron flux at *L*=6.6 for the data set during the second half of 2000 is only 0.48, the worst in all of the data sets. During the same time period, the correlation coefficient between the high-energy electron flux at *L*=6.6 and the low-middle-energy electron flux at *L*=3.5 decreases to 0.27, which means there is no relation between the two electron observations. The simple interpretation of the low correlation coefficient is the inconsistency of the two flux curves, including the shapes and widths of the peaks and valleys. The curves of the low-middle-energy and high-energy electron fluxes measured at *L*=6.6 during the second half year of 2000 are shown in Figure 3. To investigate the effect of the near-earth space environment on the behaviors of the electron fluxes, the Dst index for the same time period is also shown in Figure 3.

The third panel in Figure 3 shows that several large geomagnetic storms with Dst<–150 nT occurred during the second half of 2000. In general, the occurrence of large

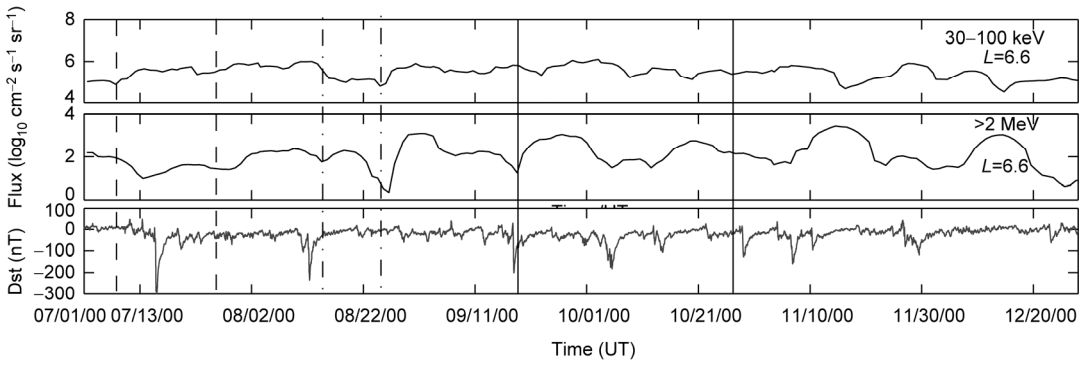

Figure 3 Comparison of the temporal variations of the electron fluxes in two different energy ranges measured at L=6.6 and the Dst index for the second half of 2000. The upper panel shows the 30–100 keV electron flux measured by POES; the middle panel shows the >2.0 MeV electron flux measured by GOES; the lower panel shows the Dst index. The electron flux curves between the two dashed lines, the two dot–dash lines and the two solid lines show the different situations of the two fluxes during different geomagnetic storms.

geomagnetic storms represents the huge energy variation in the magnetosphere, which has great influence on electron acceleration [16,17]. However, the effects of geomagnetic storms on electron fluxes are quite different for different storms. In Figure 3, between the two dashed lines, a large geomagnetic storm with Dst<–300nT occurred. Before the storm, the >2 MeV electron flux reached to a valley, following the valley of the 30–100 keV electron flux curve with a time delay of 2–3 days. After the storm, the high-energy electron flux increased slightly, in accord with the behavior of the low-middle-energy electron flux. A peak in the high–energy electron flux can be seen between the dot–dash lines. However, it is difficult to find a peak in the low-middle-energy electron flux curve within the time period between the dot-dash lines. The peaks of the low-middle-energy electron flux are about 10 days before those of the high-energy electron flux. The correlation of the electron flux curves between the two solid lines is even more abnormal—the peak of the high-energy electron flux appears prior to that of the low-middle-energy electron flux—an effect that could be due to a series of geomagnetic storms during in this period. We conclude from these observations that the correlation coefficient could be affected by some features of the electron flux curves, such as difference in the widths (durations) of peaks and valleys, the absence of peaks or valleys, or serious deformation of the curves.

Figure 4 shows the temporal variations of the low-middle-energy and high-energy electron fluxes with high correlation coefficients observed in the second half of 1999, and the Dst index for the same time period. Compared to the multiple variations in the time series of the Dst index shown in Figure 3, the space environment shown in Figure 4 is relatively quiet. Only two large geomagnetic storms occurred (between the two dashed lines and the two solid lines). It can be seen that although the variations of the low-middle-energy and high-energy electron fluxes were different during the geomagnetic storms in the second half of 1999, the time sequences of the valleys in the two electron flux curves did not change very much and therefore, neither did the correlation coefficient.

According to Figures 3 and 4, the effect of geomagnetic storms on the correlation coefficient and the best time delay between the low-middle-energy and high-energy electron flux is not clear. Based on the 1.8–3.5 MeV electron fluxes observed by the Los Alamos National Laboratory (LANL) in GEO orbit during a full solar cycle (1989–2000), Reeves et al. [18] found that 53% of geomagnetic storms result in

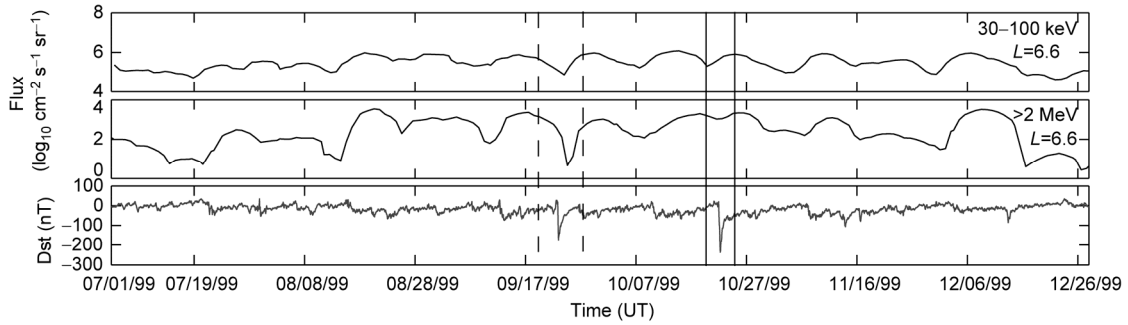

Figure 4 Comparison of the temporal variations of the electron fluxes in two different energy ranges measured at L=6.6 and the Dst index for the second half of 2000. The upper panel shows the 30–100 keV electron flux measured by POES; the middle panel shows the >2.0 MeV electron flux measured by GOES; the lower panel shows the Dst index. The two dash lines and the two solid lines indicate the electron fluxes during two large geomagnetic storms.

an increase in the high-energy electron flux, 19% of storms decrease the electron flux; and the remaining storms (28%) have little effect on electron flux. The high-energy electron flux in the magnetosphere is affected by many factors, such as the mechanisms of geomagnetic storms [19], the place where the reconnection occurs [20,21], direct high-energy electron injection [22], and the magnitude of electron loss and acceleration [23]. It is still not clear under which conditions a mechanism may dominate, or how it evolves. Another possibility is that the two electron observations from the satellites in two different orbits might cause the decrease of the correlation coefficient. The 30–100 keV electron data was obtained by the 90° detector onboard POES satellite. When the POES satellite crosses L=6.6, it is in the high latitude region, where the 90° detector is almost perpendicular to the magnetic field [24] and the electrons detected by the 90° detector are trapped particles which corresponds to the electrons with small geomagnetic equator pitch angles (about 2.5°). The detector on the GOES satellite, by contrast, is set toward the west and perpendicular to the magnetic field. The view field of the detector is 2.0sr, so the pitch angles of the electrons within >42° pitch angles can be detected by the GOES detector. As a result, the pitch angle disagreement of the two detectors onboard POES and GOES satellites could affect the measured correlation between the low-middle-energy and high-energy electron fluxes.

4.2 The variation of time delay with L value

According to the data sets with good correlation coefficients (Tables 1 and 2), the best time delays at L=5.5 are generally larger than those at L=6.6. To further understand this feature, the best time delays for these data sets are calculated from L=3.5 to L=7.0 with an interval of 0.5.

As shown in Table 4, the optimal time delays generally decrease as the L value increases. This feature implies that the local acceleration and radial diffusion mechanisms for the low-middle-energy electrons may exist simultaneously: this is because, due to the conservation of the magnetic moment for the charged particles captured by the radiation belt, the kinetic energy of electrons decreases as it diffuses from a low to high L value. Two procedures are needed for the 30–100 keV electrons at lower L values to contribute to the flux of >2.0 MeV electrons in GEO orbit (L=6.6). In the first, which employs local acceleration mechanisms, the low-middle-energy electrons at lower L values are energized to high-energy electrons. In the second, the energized electrons diffuse outward to L=6.6 and lose energy as they do so. The local acceleration mechanism should energize the low-middle-energy electrons to a high-energy, larger than 2 MeV, the smaller the L value, the larger the required energy increment. Therefore, the low-middle-energy electrons at lower L values need a longer time to be accelerated to a high-energy level. The low-middle-energy electrons at L=7.0 can reach the GEO orbit by inward radial diffusion; during this procedure, they should be energized. However, the energy increment required for the electrons at L=7.0 is much smaller than for the electrons at lower L values, so the optimal time delay for the electrons at L=7.0 is shorter.

5 Conclusions

The feasibility of building a high–energy electron forecast model by using correlation and time delay between high-energy and low-middle-energy electron fluxes has been confirmed. However, previous research used data from the same satellite only and did not consider the influence of the space environment upon the correlation. This limitation reduces the data source of the resulting forecast model. The present study, which analyzed the electron data from polar orbit satellite POES and geosynchronous orbit satellite GOES, confirmed that the correlation and time delay between low-middle- and high-energy electrons are conserved in data obtained from different orbits. Furthermore, the time delay increase with the increase of the L-value difference between the two electron observations, can be explained by local acceleration and radial diffusion mechanisms. We have also discussed the factors that affect the correlation coefficient, and shown that the correlation coefficients could be very good during the quiet period, as well as that the geomagnetic storm strongly influences the correlation coefficient.

Additional studies and new observations are needed to understand storm effects on the correlation between the low-middle- and high-energy electrons. An imaging energetic electron spectrometer (IEES) based on the pin-hole technique has been developed and tested [25,26] and can measure the pitch angle distribution of 50–600 keV electron spectrum. The launching of the IEES in the second half of

Table 4 The best time delays for the data sets with good correlation coefficients at different L values

	L=4.0	L=4.5	L=5.0	L=5.5	L=6.0	L=6.6	L=7.0
1999.01–1999.06	2.71	2.88	2.88	2.75	2.54	2.42	2.33
1999.07–1999.12	1.29	1.83	1.88	1.79	1.63	1.58	1.58
2002.07–2002.12	3.70	3.58	3.25	3.00	2.75	2.42	2.21
2003.01–2003.06	2.79	3.08	2.71	2.54	2.42	2.46	2.58
2003.07–2003.12	2.83	2.71	2.50	2.08	1.88	1.75	1.67

2016 will offer a good opportunity to investigate the correlation between low-middle-energy and high-energy electrons, as well as the acceleration mechanisms of electrons in the outer radiation belt.

This work was supported by the National Natural Science Foundation of China (Grant Nos. 41374167, 41074117 & 41374166). The authors thank the NOAA Space Weather Prediction Center for providing data from the NOAA POES satellite (http://www.ngdc.noaa.gov/stp/satellite/poes/dataaccess.html), and the National Geophysical Data Center for the solar and geomagnetic data (http://spidr.ngdc.noaa.gov/spidr/).

1 Zong Q G, Zhou X Z, Wang Y F, et al. Energetic electron response to ULF waves induced by interplanetary shocks in the outer radiation belt. J Geophys Res, 2009, 114: A10204
2 Claudepierre S G, Elkington S R, Wiltberger M. Solar wind driving of magnetospheric ULF waves: Pulsations driven by velocity shear at the magnetopause. J Geophys Res, 2008, 113: A05218
3 Zong Q G, Wang Y F, Yuan C J, et al. Fast acceleration of "Killer" electrons and energetic ions by interplanetary shock stimulated ULF waves in the inner magnetosphere. Chin Sci Bull, 2011, 56: doi: 10.1007/s11434–010–4308–8
4 Yan Q, Shi L Q, Liu S Q. Effect of seed electron injection on chorus-driven acceleration of radiation belt electrons. Sci China Tech Sci, 2013, 56: 492–498
5 Ding Y H, He Z G, Zhang Z L, et al. Influence of wave normal angle on gyroresonance between chorus waves and outer radiation belt electrons. Sci China Tech Sci, 2013, 56: 2681–2689
6 Wang D D, Yuan Z G, Deng X H, et al. Compression-related EMIC waves drive relativistic electron precipitation. Sci China Tech Sci, 2014, 57: 2418–2425
7 Selesnick R S, Blake J B, Kolasinski W A, et al. A quiescent state of 3 to 8 MeV radiation belt electrons. Geophys Res Lett, 1997, 24: 1343–1346
8 Li X L, Temerin M, Baker D N, et al. Quantitative prediction of radiation belt electrons at geostationary orbit based on solar wind measurements. Geophys Res Lett, 2001, 28: 1887–1890
9 Barker B, Li X, Selesnick R S. Modeling the radiation belt electrons with radial diffusion driven by the solar wind. Space Weather, 2005, 3: S10003, doi:10.1029/2004SW000118
10 Drew L, Turner W, Li X L. Quantitative forecast of relativistic electron flux at geosynchronous orbit based on low-energy electron flux. Space Weather, 2005, 6: S05005
11 Lam, H L. On the prediction of relativistic electron fluence based on its relationship with geomagnetic activity over a solar cycle. J Atmos Sol-Terr Phy, 2004, 66: 1703–1714
12 Nagai T. "Space weather forecast": Prediction of relativistic electron intensity at synchronous orbit. Geophys Res Lett, 1988, 15: 425–428
13 Paulikas G A, Blake J B. Effects of the solar wind on magnetospheric dynamics: Energetic electrons at the synchronous orbit, quantitative modeling of magnetospheric processes 21. Geophys Monograph Series, 1979, 79: 180–202
14 Li X L, Baker D N, Temerin M,et al. Energetic electrons, 50 keV to 6 MeV, at geosynchronous orbit: Their responses to solar wind variations. Space Weather, 2005, 3: S04001
15 Lam M M, Horne R B, Meredith N P, et al. Moffat–Griffin T and Green J C, Origin of energetic electron precipitation >30 keV into the atmosphere. J Geophys Res, 2010, 115: A00F08
16 Geoffrey D. Reeves, relativistic electrons and magnetic storms: 1992–1995. Geophys Res Lett, 1998, 25: 1817
17 Dmitriev A V, Chao J K, Dependence of geosynchronous relativistic electron enhancements on geomagnetic parameters. J Geophys Res, 2014, 108: 1388
18 Reeves G D, McAdams K L, Friedel R H W, et al. Acceleration and loss of relativistic electrons during geomagnetic storms. Geophys Res Lett, 2003, 30: 1529
19 Denton M H, Borovsky J E, Skoug R M, et al. Geomagnetic storms driven by ICME- and CIR-dominated solar wind. J Geophys Res, 2006, 111, doi: 10.1029/2005JA011436
20 Le G, Russell C T, Gosling J T, et al. ISEE observations of low latitude boundary layer for northward interplanetary magnetic field: implications for cusp reconnection. J Geophys Res, 1996, 101: 27239–27249
21 Paschmann G, Sonnerup BUÖ, Papamastorakis I, et al. Plasma acceleration at the Earth's magnetopause: evidence for reconnection. Nature, 1979, 282: 243–246
22 Hasegawa H, Fujimoto M, Phan T D, et al. Transport of solar wind into Earth's magnetosphere through rolled-up Kelvin-Helmholtz vortices. Nature, 2004, 430: 755–758
23 Friedel, R H W, Reeves G D, Obara T. Relativistic electron dynamics in the inner magnetosphere: A review. J Atmos Sol-Terr Phy, 2002, 64: 265–282
24 Rodger, C J, Clilverd M A, Green J C, et al. Use of POES SEM–2 observations to examine radiation belt dynamics and energetic electron precipitation into the atmosphere. J Geophys Res, 115, 2010, A04202
25 Zou H, Luo L, Li C F, et al. Angular response of 'pin-hole' imaging structure measured by collimated source. Sci China Tech Sci, 2013, 56: 2675–2680
26 Luo L, Zou H, Zong Q G, et al. Anti–proton contamination design of the imaging energetic electron spectrometer based on Geant4 simulation. Sci China Tech Sci, 2015, 58: doi: 10.1007/s11431–015–5863–7